3 REGIONAL HYDROLOGY

P.E.V. van Walsum, F.J.E van der Bolt, and A.A. Veldhuizen

3.1 Introduction

The focus of this study is on predicting effects involving interactions at or near the soil surface and in the waterways that form the surface water system. It is therefore a logical choice to use a regional hydrologic model of the comprehensive type, and not a model that for instance covers only groundwater. Comprehensive models that describe all aspects of the regional system in great detail have, however, the disadvantage that they are computationally very intensive and allow only the simulation of short time periods. An example of such a model is the SHE model (Abbot *et al*. 1986). When studying the impacts of climate change it is of paramount importance that long periods can be simulated, because 'climate' is defined for periods that span 20-30 years. And for coming to grips with statistics of events with a recurrence interval of for instance 5 years, it is also important to be able to simulate long enough periods. For this reason and for the fact that the model has specific options suitable for describing the special aspects of lowland hydrology, the choice was made to use the model SIMGRO (Veldhuizen *et al*., 1998). SIMGRO covers all relevant aspects of the regional hydrologic system, but does so in a manner that allows the simulation of long time periods, even for models of a mid-sized drainage basin. This has been achieved by setting integration above detail in the model conception. Figure 3.1 and Figure 3.2 give a general idea about SIMGRO and the way that it covers the regional hydrology.

We will describe various aspects of this model in more depth as we describe its implementation for the study region. For a comprehensive description of the model the reader is referred to Veldhuizen *et al*. (1998).

Figure 3.1 Schematization of water flows in SIMGRO, by means of transmission links and storage elements.

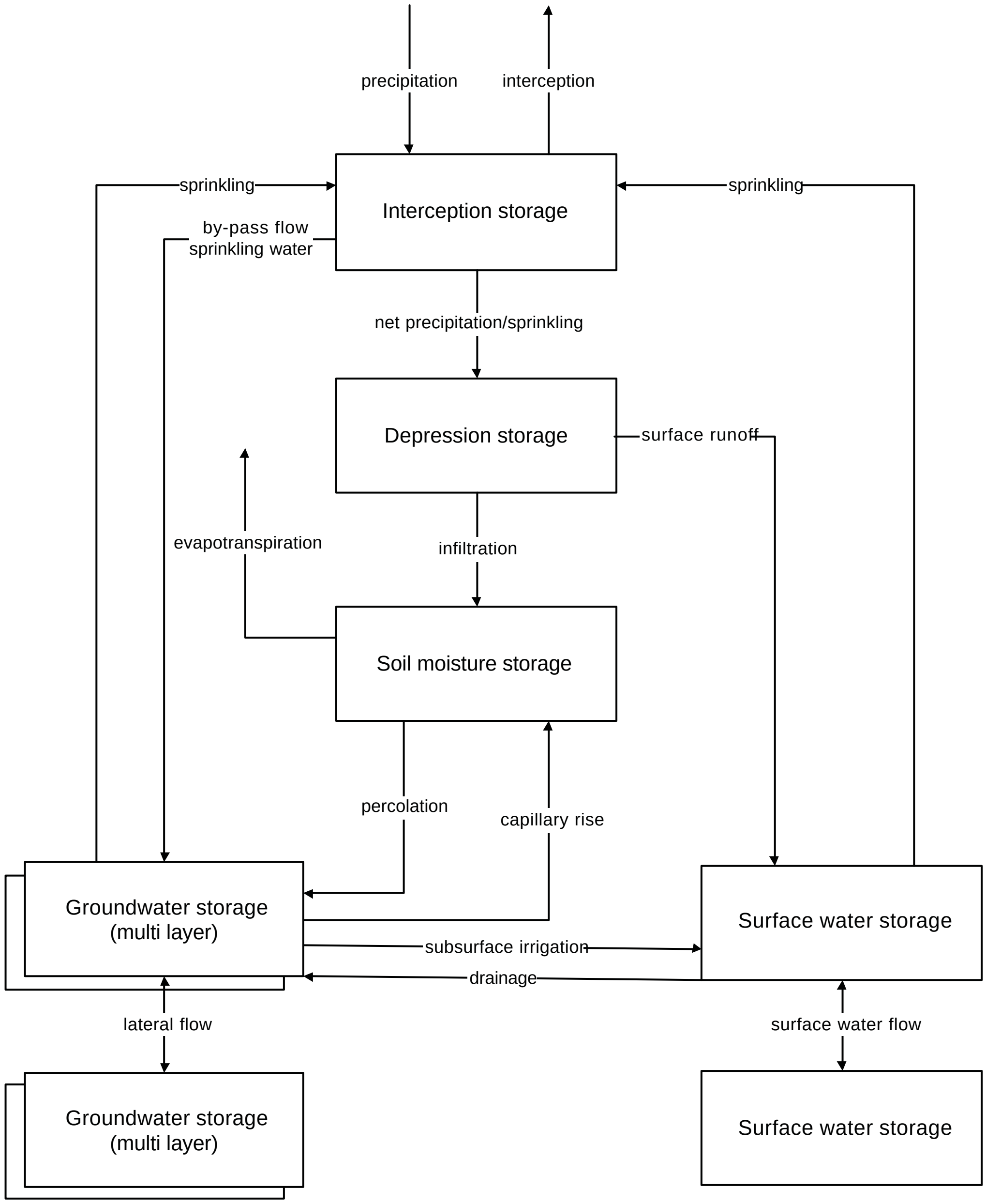

Figure 3.2 Schematization in SIMGRO of the hydrological system within a nodal subdomain by means of an integration of saturated zone, unsaturated zone and surface water (Querner and Van Bakel 1989).

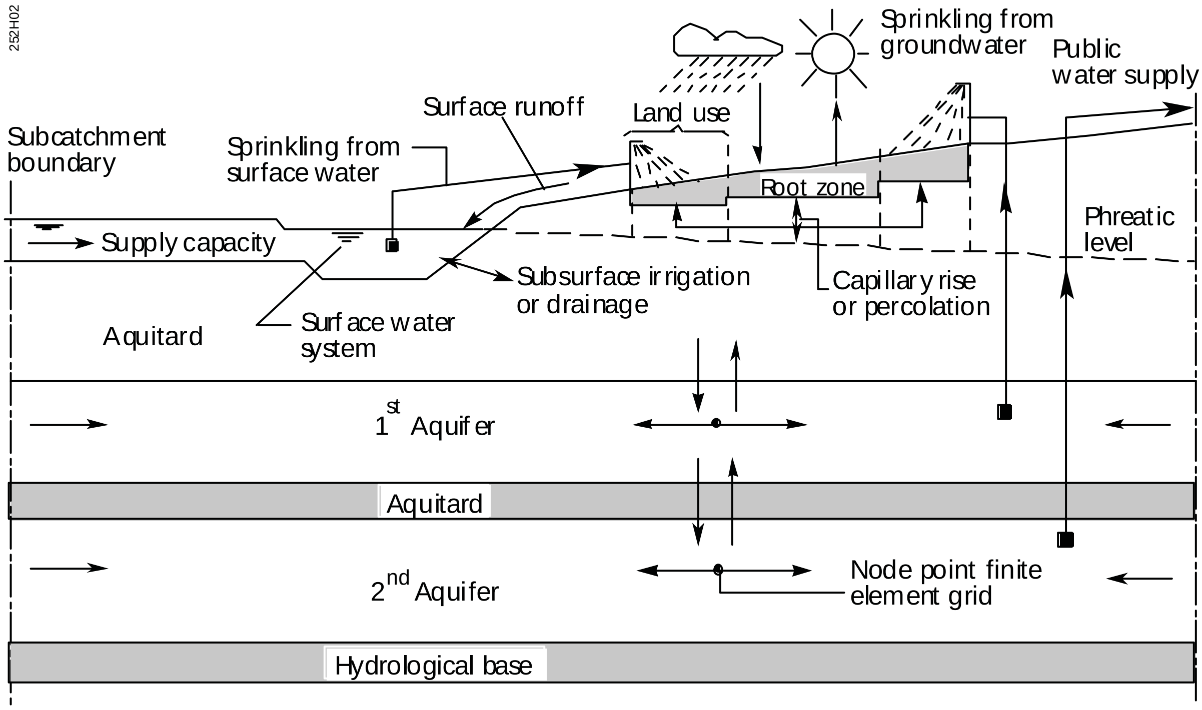

3.2 Implementation of SIMGRO for the study region

3.2.1 Spatial discetisation and time steps

SIMGRO has a finite-element discretisation of the regional domain for describing the spatial aspects. Constructing triangles between nodes forms the finite elements. For each node a so-called nodal subdomain can be geometrically inferred. For the study region there are 12 000 nodes that form about 25 000 triangles. This spatial discretisation covers a larger area than the study region, in order to avoid gross inaccuracies near the borders. Thus the 'model region' covers some 67 000 ha, whereas the 'study region' roughly covers 45 000 ha. Along the main streams the distance between the nodes has been made smaller (100 m) in order to model the processes along the stream valleys more accurately. This is especially important for modelling inundation processes and for computing the seepage that is ecologically relevant. If the distance between the nodes is chosen too large, then the seepage in the stream valleys is averaged out. The consequence of this averaging out is that the reaching of critical thresholds is not predicted correctly.

The groundwater and surface water submodels of SIMGRO each run with a time step that is tuned to the type of dynamic behavior. The groundwater submodel has a time-step of 0.25 day and the surface water submodel has a time step of 0.025 day. Model output of the surface discharges are however integrated and averaged over the time period of one whole day, because the dimensioning of water channels in the Netherlands is based on the frequency distribution of such daily averages.

3.2.2 Groundwater

Schematisation of the subsoil

The groundwater flow in the subsoil is modeled using a schematization into layers involving horizontal flow, the aquifers, interspersed by layers involving only vertical flow, the aquitards. The used schematisation has been provided by NITG-TNO through their REGIS system (NITG-TNO 1994a). The schematisation involves in total 15 layers, which are described in Table 3.1. As can be seen from the table several of the formations have been split into an aquifer and an aquitard. For each of the layers the REGIS-system has provided a map of the conductivity and a map of the layer thickness. An example of a map of the conductivity is given in Figure 3.3, which shows the conductivity of the Sterksel/Nuenen coarse layer, the layer that plays a crucial role in determining conditions near the soil surface.

Table 3.1 Schematisation of the subsoil of the study region Beerze & Reusel, provided by NITG-TNO through the REGIS database (NITG-TNO 1994a).

Layer	Formation	Type
1	Nuenen fine sand	aquifer
2	Nuenen loam	aquitard
3	Sterksel/Nuenen coarse	aquifer
4	Kedichem/Tegelen clay	aquitard
5	Kedichem/Tegelen fine sand	aquifer
6	Tegelen clay	aquitard
7	Tegelen gravel	aquifer
8	Maassluis/Belfeld clay	aquitard
9	Belfeld gravel	aquifer
10	Kallo/Reuver clay	aquitard
11	Schinveld sand	aquifer
12	Oosterhout,/Brunssum clay	aquitard
13	Zanden van Pey	aquifer
14	Brunssum clay	aquitard
15	Waubach sand	aquifer

Figure 3.3 Example of a map of the subsoil conductivity, provided by NITG-TNO through the REGIS-database for the 'Sterksel/Nuenen coarse' layer (layer 3, Tabel 3.1)

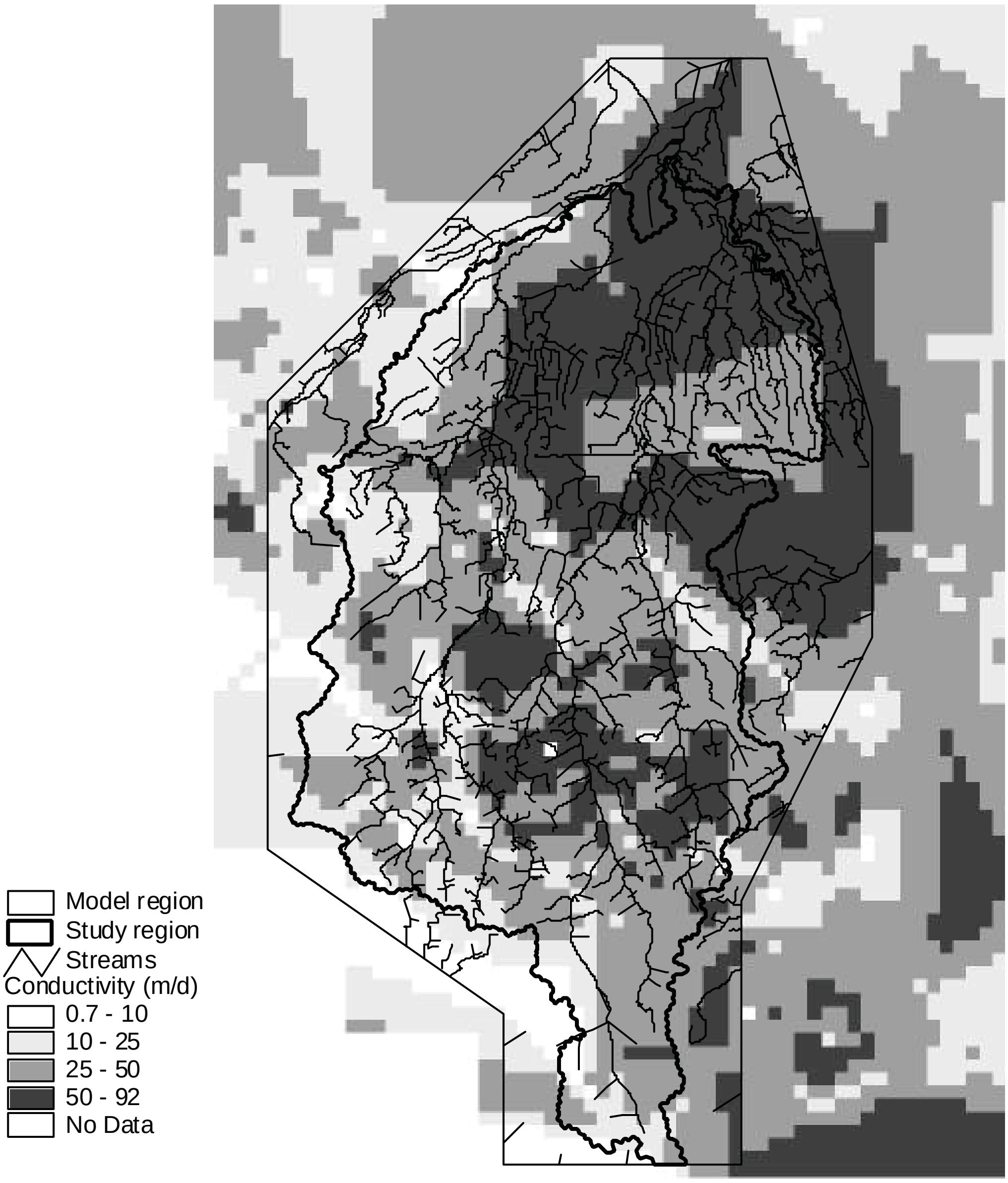

Boundary conditions and groundwater extractions

For being able to simulate the regional groundwater flow it is necessary to have information about the conditions along the boundary of the model region. For very large drainage basins the flux along the border can be set to zero without making significant errors. However, for an intermediate-size basin it is of great importance to get as accurate as possible information. Preferably this information should concern a boundary condition of the 'third kind', which gives a relationship between the head at the boundary and the flux across it. Like in most cases such information is not available. So instead information about the groundwater head has been used, from the following two sources:

- the NAGROM model for the Netherlands (De Lange 1991)
- the OLGA database (NITG-TNO 1994b)

The NAGROM-model has the advantage that it covers all depths along the boundary, even though there are less layers (6) than the 15 layers of the REGIS schematisation. The dis-advantage of NAGROM is, however, that it is steady state. It is known that during the last

Figure 3.4 Time series of groundwater heads at OLGA-measurement station 57AP0025, depth of filter at –44 m+NAP. The time series has been used for superimposing the yearly and long-term trend of deep groundwater heads on the steady-state boundary conditions provided by NAGROM.

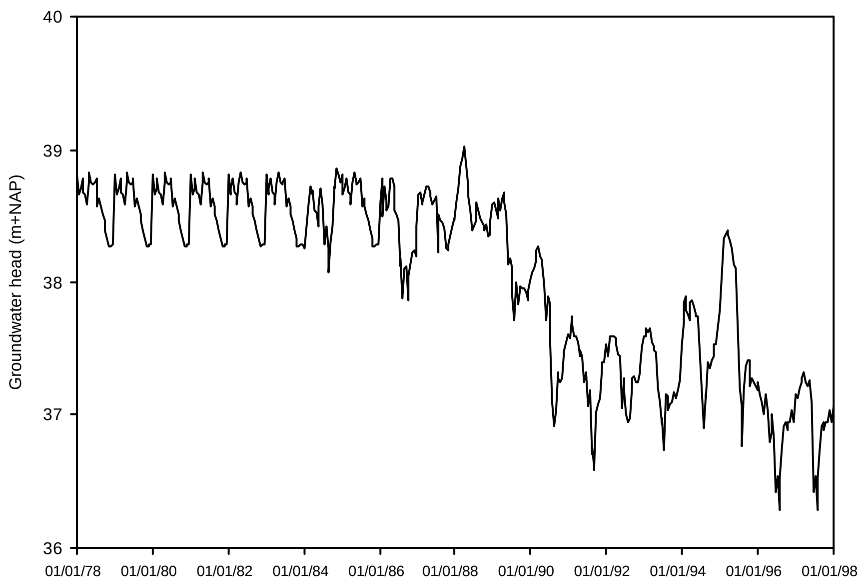

decade a sharp decrease of watertables has steadily been taking place. Also within the years themselves there are variations according to the seasons. In order to take both these long-term and annual changes into account we have used a measuring well thought to behave in a way that is representative for the regional system and have superimposed the fluctuations on the information provided by the NAGROM-model. The used series is shown in Figure 3.4.

In the region there are substantial extractions for drinking water supply and industry: these extractions total 25.5 million m^3/yr, which for a total model region of 67 000 ha is about 37 mm/yr. The main extraction is 8.5 million m^3/yr and is located just outside the study region on the eastern side.

3.2.3 Soil water and plant-atmosphere interactions

Schematisation, land use and evapotranspiration

The dynamics of soil water are modeled as vertically oriented, one-dimensional models. Per nodal subdomain the dominant land use is determined for being modeled. The main forms of land use are tabulated in Table 3.2 .

Table 3.2 Types of land use in the study region (only types with an area >1% have been tabulated).

Type of land use	Area (% of region)
grassland (agriculture)	46.6
maize	13.6
potatoes	2.6
beets	1.1
horticulture	1.9
deciduous forest	3.8
coniferous forest	17.6
heather	1.0
natural grassland	2.1
built-up area	4.9
grass in built-up area	2.1
rest	2.7
total	**100.0**

Evapotranspiration is computed in two steps:

- computation of the potential evapotranspiration by multiplying the Makkink reference crop evapotranspiration by a crop-specific factor
- computation of the actual evapotranspiration by (if necessary) reducing the evapotranspiration in situations with a moisture deficit

This method is described in Feddes (1987).

Water balance of the unsaturated zone and the shallow groundwater

The 1-D column model consists of two reservoirs, one for the root zone and one for the subsoil. If the equilibrium moisture storage for the root zone is exceeded, excess water will percolate to the saturated zone. If the moisture storage is less than the equilibrium moisture storage, upward flow from the saturated zone is simulated through capillary rise. The height of the phreatic surface is calculated from the water balance of the subsoil, using a storage coefficient that is dependent on the depth of the watertable. This function for the storage coefficient is derived by making a sequence of calculations with the steady-state model CAPSEV of the unsaturated zone (Wesseling 1991).

Storage of water on the soil surface

For modelling situations with inundation it is necessary to simulate the storage of water on the soil surface. This is done in SIMGRO using an inundation curve giving the relationship between the watertable and the fractional area of a nodal subdomain that is inundated. This inundation curve is added to the storage coefficient for the unsaturated zone, yielding an integrated water storage curve for the phreatic watertable. In this way inundation is modeled as ‘visible groundwater’.

3.2.4 Surface water

Schematisation

In the Netherlands, the surface water system often consists of a dense, complex network of water conduits with lots of hydraulic features. In a simulation model at regional scale like SIMGRO it is not feasible to explicitly account for all these conduits and their interconnections individually (Querner and Van Bakel 1989). For this reason only the larger conduits are explicitly included in the schematisation. The smaller ones area assumed to be equally distributed over the nodal subdomain that they are within. So only the first two classes of conduits are explicitly modeled of the 5 classes that are distinguished in SIMGRO. These 5 classes are:

- 1^{st} order conduits: rivers, canals
- 2^{nd} order conduits: large streams, large brooks
- 3^{rd} order conduits: small streams, small brooks, ditches
- 4^{th} order conduits: drain pipes, collector drains
- 5^{th} order conduits: trenches, furrows, soil surface

In this classification the 5^{th} order is of special interest. This order of conduits is used in the model to also model the soil surface: when the groundwater rises to the soil surface the soil surface itself starts to act as a drain. This process is of special relevance to this study, because the drainage over the soil surface is one of the main causes of high discharges under extremely wet conditions.

The water levels in the conduits that are explicitly modeled (1^{st} and 2^{nd} order) are assumedly propagated to the smaller conduits within a subcatchment. The SIMGRO model has various options for representing this. The basic ones are:

- propagation parallel to the soil surface;
- propagation on a horizontal plane

The first option applies to conditions that normally prevail in agricultural areas without weirs. In those areas the surface water network will generally have been dimensioned in such a manner that the discharge capacity is tuned to the circumstances. The latter option is usually relevant in case there is a weir, or under conditions involving infiltration and/or inundation.

In the study region the structure of the surface water network was derived from data supplied by the waterboard. Intensive data-analysis and correction procedures were needed to bring the data into order. In the data-processing procedure the streams and canals were also divided into 2350 subtrajectories of at most 500 m, which was needed for the modelling.

Interaction between groundwater and surface water

The interactions between groundwater and surface water are simulated for each nodal subdomain. A drainage/infiltration flux is computed per order of surface water conduits by dividing the difference in head through the drainage resistance. Fluxes are only computed for conduits that are ‘active’. A conduit is active if one of the following conditions is met (or both):

- the watertable is above the bottom of the conduit
- the surface water level is above the bottom of the conduit

The drainage resistance is considered to have three components:

- the resistance involved in transporting drainage water horizontally towards the conduit, which is computed with a conventional drainage formula (see Veldhuizen *et al*. 1998)
- the resistance involved in the radial flow in the direct vicinity of the conduit
- the resistance involved in the entrance to the conduit, caused by loamy material in the conduit walls

In practice it is hard to distinguish between the latter two types of resistance. They therefore are usually combined into a composite resistance γ_r. It has been found that a value of 0.8 d/m is a good first guess for it. The actual drainage resistance is then found by multiplying this resistance by the mean distance between the conduits:

$$\gamma = \gamma_r \cdot L + \gamma_h \qquad (3.1)$$

in which:

- γ : drainage resistance (d)
- γ_r: radial/entrance resistance (d/m)
- L : mean distance between conduits (m)
- γ_h : ‘horizontal’ drainage resistance (d/m)

The mean distance between conduits is found by dividing the area of a nodal subdomain by the sum of the lengths of the conduits, assuming that the conduits are equally distributed over the nodal subdomain:

$$L = A / \Sigma\, l \qquad (3.2)$$

in which:

- $\Sigma\, l$: sum of lengths of a conduit of a certain order (m)
- A : area of a nodal subdomain (m^2)

Figure 3.5 Drainage resistance of trenches/furrows as a function of the fractional inundation.

A fractional inundation of 0.50 corresponds with a watertable equal to the average soil surface elevation in a nodal subdomain.

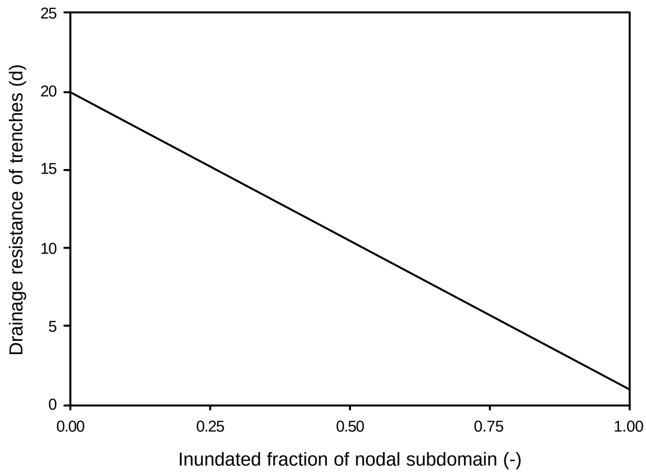

In the computation of the drainage resistance for the larger conduits the mean distance L soon becomes larger than the cross-section of a nodal subdomain. In that case not L is used, but the cross-sectional distance of the nodal subdomain. This provision is necessary to avoid double counting of horizontal resistances in the model: the groundwater flow between the nodes themselves is computed with the finite element scheme.

The 5^{th} order drainage plays a special role in the model, because it is also used for modelling the surface runoff that occurs when the groundwater reaches the soil surface. In the case of total inundation the flow resistance becomes small. The resistance has therefore been made dependent on the degree of inundation. On the basis of past experience we have set the value for complete inundation at 1 d. For fractions of inundation between 0.0 and 1.0 the resistance is varied linearly, starting from 20 d for situations with no inundation (Figure 3.5).

Dynamics of surface water

The surface water system is modeled as a concatenation of reservoirs, each one controlled at the outlet by a weir or an imaginary one, using a tabulated Q-h relation. This Q-h relation implicitly accounts for all hydraulic features within the reservoir in a 'black box' manner. That includes also the conditions at bifurcations, of which there are about 10 in the study region. Bifurcations are present at places where the waterboard has made a parallel conduit – which then becomes the new main stream – to reduce the inundations around the old main stream.

3.3 Calibration

3.3.1 Introduction

Even for a ‘physically based’ model like SIMGRO some form of calibration is inevitable. In the current practice of groundwater modelling the use of automated parameter fitting procedures is becoming more and more prevalent. An example of a much used software package is PEST (Dougherty 2000). Such software has, however, not been used in the current study. There are various reasons for this. Firstly, the running of the SIMGRO model used in this study (12 000 nodes, 15 layers) takes roughly an hour of CPU-time per year of simulation. For purposes of automated fitting that is very unwieldy. Secondly, we did not only use head data, but also looked at the discharges. That makes it hard to find a suitable goal function. Thirdly, even with the use of automated procedures one can not escape from specifying the bounds for realistic values of parameters. That usually is done manually anyhow, largely determining the outcome of the calibration.

It is also the opinion of the authors that the use of automated calibration methods does not at all guarantee that the produced results are better than when the calibration is done ‘by hand’. At most automated calibration methods can reduce the amount of time involved in the calibration process. The geostatistical interpretation of the parameter covariances that are computed is extremely hazardous if not all of the relevant system parameters are taken into account.

3.3.2 Available data and calibration criteria

The following sources of data have been used:

- a map of the Mean Highest Watertable (Kleijer *et al*. 1990)
- a map of the Mean Lowest Watertable (Teunissen van Manen 1985)
- data of watertable gauging wells registered in the OLGA-database (NITG-TNO 1994b)
- discharge measurements of the Reusel and the Beerze
- amounts of sprinkling in the Hilver land reconstruction area (Van der Bolt *et al*. 1999)

In the Netherlands maps of Mean Highest Watertable (MHW) and Mean Lowest Watertable (MLW) are widely used for characterizing the groundwater regime. The definition of the Mean Highest Water table is as follows:

- from a series of gauged watertables on the 14^{th} and 28^{th} day of each month the three highest levels are selected for each of the gauging years
- per gauging year the average of the three selected levels is taken, yielding the so-called HG3-level for each of the available years
- the HG3-levels are averaged over the years, yielding the MHW-value

The revised map of the MHW for 1990 is given in Figure 3.6a. Even though this map is fairly recent, it should be realized that in the past ten years changes have taken place causing further desiccation in the region (Figure 3.4). The Mean Lowest Watertable is derived in a similar fashion. The map given in Figure 3.6b has been made by the former soil survey institute STIBOKA in the early 1980's (Teunissen van Manen 1985). More than 20 years have gone by since it was made, so this map is out of date. But in practice the map of MLW is less susceptible to change than the one of MHW, so the available map of MLW still contains valuable information.

Only limited information is available on the amount of sprinkling in the region. According to a survey done for the rural reconstruction project Hilver (Van der Bolt *et al*. 1999) the average amount of sprinkling is roughly 16 mm per year, averaged out over the gross area (including non-agricultural areas).

Comparisons between calibration runs have been made through visual means, using maps (watertables) and exceedance frequency curves (discharges), and through using numerically defined criteria. For comparing the simulated and measured maps of Mean Highest and Mean Lowest Watertable the calibration criteria are in terms of class differences. Use had to be made of classes because the measured maps are only available in that form. For instance for the Mean Highest Watertable the following function has been used:

$$E_{MHW} = (1 - \Sigma \mid MHW_m - MHW_s \mid / N) \cdot 100\% \qquad (3.3)$$

in which:

- E_{MHW} : model efficiency for simulating the Mean Highest Water table (%)
- MHW_m : class of measured Mean Highest Watertable for a pixel (-)
- MHW_s : class of simulated Mean Highest Watertable for a pixel (-)
- N : number of pixels

So if the average deviation is one class, the computed efficiency is zero.

For the discharges the following statistics have been used:

- average flow difference, Δq (% of mean discharge)
- goodness of fit, E_q (%)

The used 'goodness of fit' criterium for the discharges is the well-known function proposed by Nash & Sutcliffe (1970):

$$E_q = (1 - \Sigma\,(q_m - q_s)^2 / \Sigma\,(q_m - q_{m,a})^2\ ) \cdot 100\% \quad (3.4)$$

Figure 3.6a The Mean Highest Watertable for the study region (Kleijer *et al*. 1990)

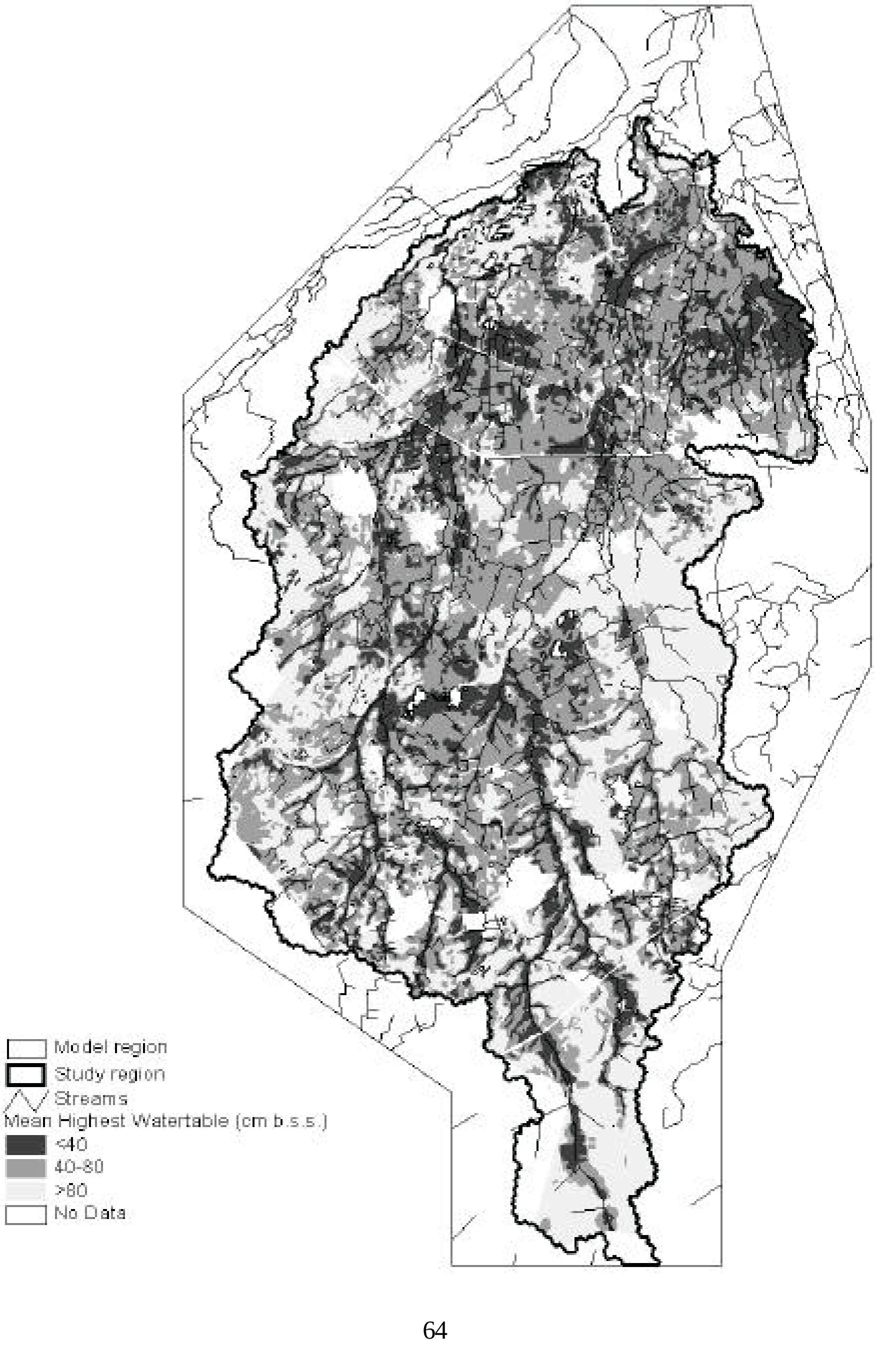

in which:

- E_q : model efficiency for simulating discharges (%)
- q_m : measured discharge (l/s)
- $q_{m,a}$: average measured discharge (l/s)
- q_s : simulated discharge (l/s)

Figure 3.6b Map of Mean Lowest Watertable (Teunissen van Manen 1985).

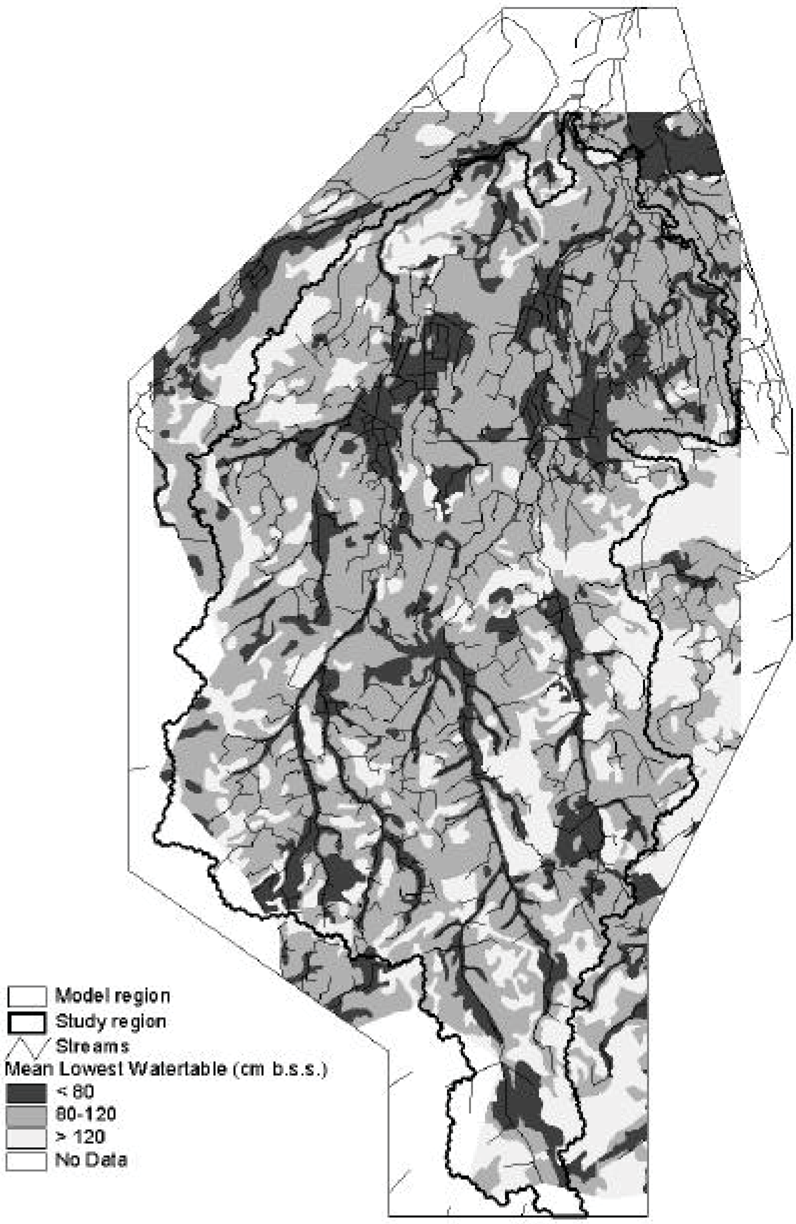

3.3.3 Results for the uncalibrated model

The results for the uncalibrated model are shown in the form of the Mean Highest Watertable MHW in Figure 3.7 and the exceedance frequencies of the simulated and measured discharges of the Beerze and the Reusel in Figure 3.8. The run with the model was done for 1980-90, i.e. the same period as of the available MHW-map. The following calibration criteria values were found:

- E_{MHW} = 52%; E_{MLW} = 80%
- $E_{q,R}$ = 58% (Reusel); $E_{q,B}$ = 75% (Beerze)

Figure 3.7 Map of the Mean Highest Watertable, simulated by the uncalibrated model. Downscaling is done using the procedure described in Section 5.2

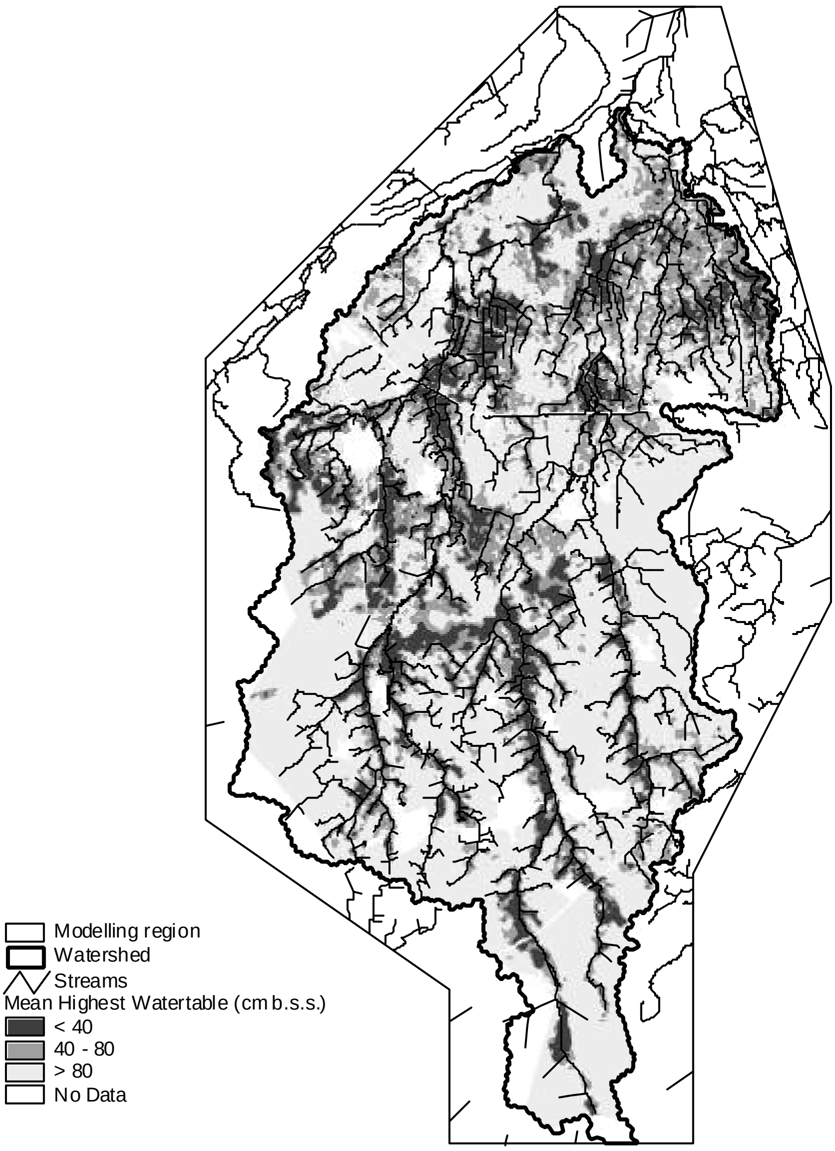

Figure 3.8 Exceedance frequency curves for discharges of the Beerze and Reusel, simulated by the uncalibrated model.

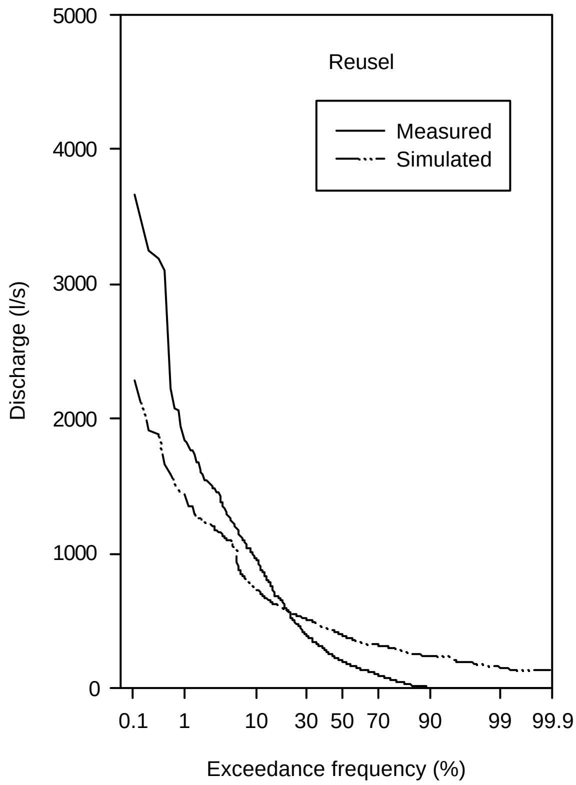

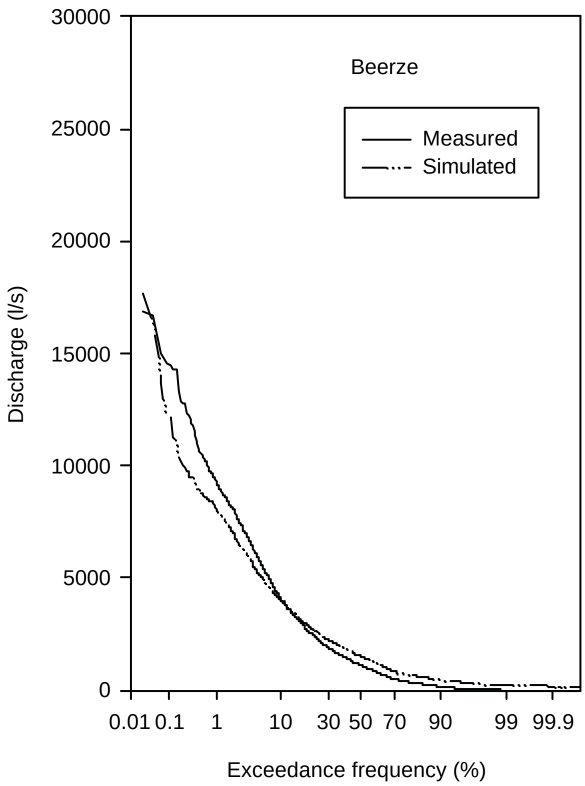

Comparison of the simulated and measured maps of the Mean Highest Watertable shows that the errors are mainly made along the flanks of the valleys: the simulated maps show an abrupt change from very wet conditions to very dry ones, whereas the measured map shows that also higher up on the valley slopes a large percentage of the area remains in the second class with Mean Highest Watertables between 40 and 80 cm b.s.s. (cm below soil surface). A visual inspection of the discharge exceedance frequency curves shows a big difference in behavior for the Reusel. The simulated peak discharges are far lower than the measured ones, and the low flows continue much longer in the model than in reality.

3.3.4 Adjustment of parameters

Preliminary analysis of main parameters to be calibrated

Initially the sprinkling capacity was set to 1.00 mm/d for all agricultural crops. The computed long-term average of the sprinkling amount was found to be 24 mm/yr, if the sprinkling is averaged out over the whole region. That is 1.5 times the 16 mm/yr found in the Hilver rural reconstruction area (Van der Bolt *et al*. 1999). For this reason the sprinkling capacity of crops was lowered to 0.67 mm/d.

The next calibration question concerns the main cause of the differences between measured and simulated data: are they caused by the geohydrological parameters of the subsoil, the drainage resistances, or other parameters? To investigate the influence of the drainage resistances a calibration run was made with all the entry resistances of streams, ditches and drains set to 4.0 d, which is extremely high. The result for the simulated map of the Mean

Figure 3.9 Map of the Mean Highest Watertable, simulated after setting the entry resistances of the streams, ditches and drains at 4.0 d (extremely high).

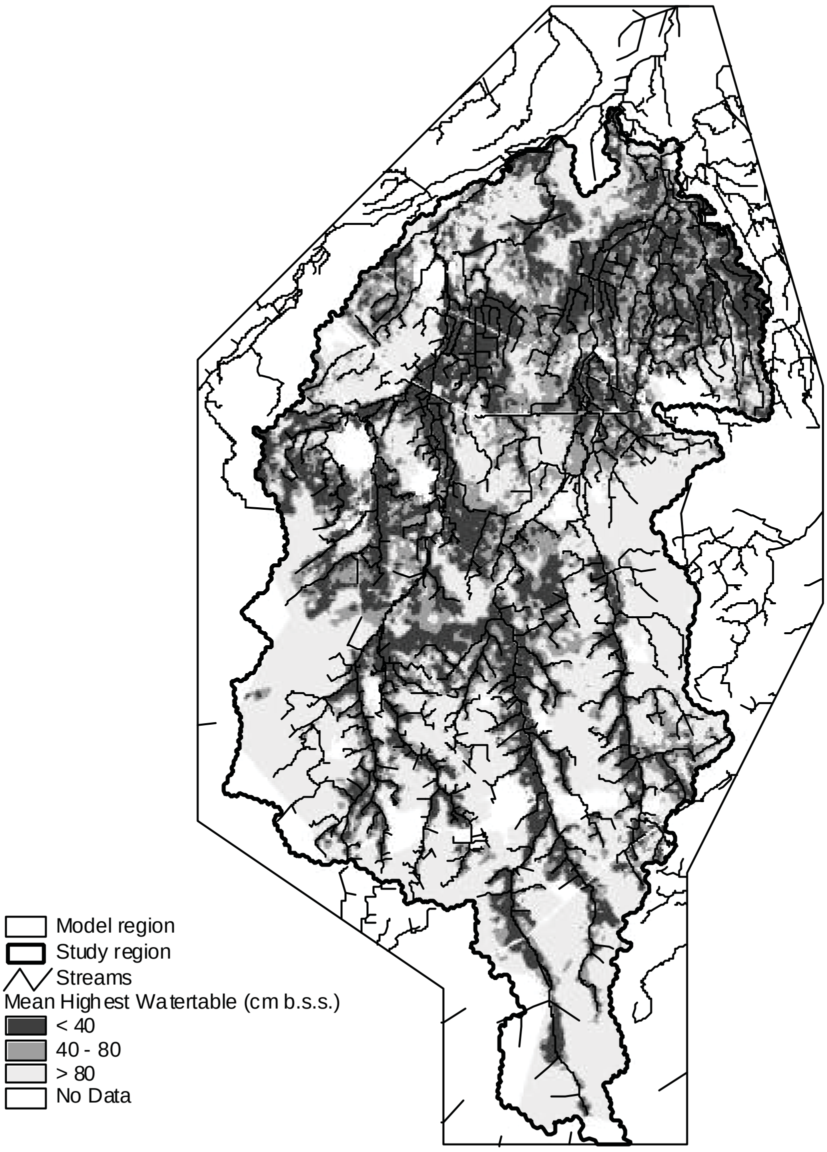

Highest Watertable is shown in Figure 3.9. As can be seen from the map the simulated conditions in the stream valleys become even more wet, whereas the conditions on the higher grounds along the stream valleys are still too dry. The reason for this local effect on the conditions along the streams is that the drainage resistances are only active in the model nodes where the groundwater is above the bottoms of the waterways, which is at the bottom of the valleys. Increasing the resistances causes the groundwater to reach the soil surface along the streams, because the soil surface is the only remaining route for the water to leave the groundwater system and enter the stream, since the other resistances have been set very high. The effect of setting the drainage resistances very high is also reflected in the computed criteria for the Mean Highest and Mean Lowest Watertable:

- E_{MHW} = 58% (was 52%)
- E_{MLW} = 74% (was 80%)

On the basis of the criterium E_{MHW}, the similarity between simulated and measured maps has become better, but judged ‘visually’ the pattern has decidedly become a worse fit. Also the similarity with respect to the Mean Lowest Watertable has become worse. In conclusion, sharply increasing the drainage resistances is not the right course of action to improve the model.

From the above computational experiment it has become clear that the drainage resistances are not the main cause for the differences between measured and simulated variables. Instead, the images of the simulated watertables indicate that the initial estimates of the geohydrological conductivities are far too high. Owing to these high values the groundwater can flow without much of a gradient towards the valleys, to where the streams are. This leaves the valley flanks high and dry. Inspection of the geohydrological data revealed that for instance the conductivities of the first layer – modeled as an aquifer – range between 2 and 100 m/d. Considering that this concerns fine-sandy sediments, such a range seems to be unrealistic. Values of up to a maximum of 5-20 m/d are what one would expect. Also the initial estimates of the third layer – the Formation of Sterksel – seem to be unrealistically high: the conductivity ranges between 0.7 and 92 m/d, with 75% of the values higher than 25 m/d. This formation is reputed to have conductivities between 20 and 30 m/d (Negenman *et al*. 1998). So both information from other sources about the conductivities themselves and also the initial results of the uncalibrated model pointed towards the necessity of lowering the conductivity values in the course of the calibration.

After having performed the above preliminary analysis, the following stepwise calibration procedure was decided upon:

- adjustment of geohydrological parameters of shallow layers (1 through 4)
- adjustment of drainage resistances of main waterways and streams
- adjustment of drainage resistances of field ditches and drains
- adjustment of trench resistances

Adjustment of geohydrological parameters of the shallow layers

The following modifications were made (the numbering corresponds to the numbers of calibration runs in Table 3.3):

- the conductivity of the first layer was reduced through the operation $k' = 2*\sqrt{k}$; by taking the square root most of the reduction is on the high values, whereas the lower values are modified less; this does not change the regional pattern of watertables very much, however (calibration run 3 of Table 3.3)
- in the south-western quarter of the study region (the higher ground in the Reusel basin) a resistance was introduced in the second layer of 3000 d, and the kD-value of the top layer was set to 4 m^2/d (thickness of 4 m and a conductivity of 1 m/d) (run 4)
- in the southern half of the region (to the south of the so-called Feldbiss fault) a resistance of 2000 d was introduced in the fourth layer (run 5)
- the conductivity of the Sterksel Formation (layer 3) was reduced through the operation $k' = 3*\sqrt{k}$; this brings the range of conductivities within the 0-30 m/d interval reported by Negenman *et al.* (1998) (run 6)

The results for the calibration criteria are summarized in Table 3.3, runs 3 – 6. As can be seen from the table, the efficiency criterium for the Mean Highest Watertable is substantially improved, without hardly decreasing the efficiency criterium for the Mean Lowest Watertable.

Adjustment of drainage resistances

On the basis of field knowledge and the density of the waterways it was concluded that in the northern part of the study region there must be relatively more loamy material in the shallow subsoil than in the southern half. It was therefore decided to differentiate the entry resistance

Table 3.3 Values of calibration criteria for the calibration runs. E_{MHW} and E_{MLW} : efficiency parameters for the fit of the Mean Highest and Mean Lowest Watertable; $E_{q,R}$ and $E_{q,B}$: efficiency parameters for the simulated discharges of Reusel and Beerze. The mean flows are evaluated in terms of the percentage difference between simulated and measured (positive values mean that the simulation is higher).

Run	Short description of calibration run	E_{MHW} (%)	E_{MLW} (`%)	$E_{q,R}$ (%)	$E_{q,B}$ (%)	Δq_R (%)	Δq_B (%)
1	Initial estimate	51.7	79.6	58.1	75.1	29.1	12.3
2	High drainage resistances waterways	58.2	73.5	62.2	78.0	21.9	6.8
3	Reduction of 1st layer conduct. k'=2*√k	52.7	79.2	59.3	75.5	26.9	11.1
4	Resistance 2nd layer 3000d, southwest	54.6	79.0	65.9	75.6	21.5	10.5
5	Resistance 2000d 4th layer, south	54.6	79.1	65.8	75.4	22.0	10.5
6	Reduction of 3rd layer conduct.k'=3*√k	55.9	79.1	66.4	74.7	22.9	7.7
7	Increase of entry resistance of streams in northern half from 0.8 d to 1.2 d.	56.5	79.0	66.4	74.7	22.8	7.5
8	All entry resistance streams +25%	56.8	78.7	66.6	74.8	22.5	7.2
9	All entry resistances streams +60%	57.1	78.3	67.0	74.9	21.9	6.6
10	Agricultural drainage included	58.2	79.5	68.2	75.1	23.2	7.4
11	Resistance of trenches 10 d	58.2	79.5	69.3	75.2	23.1	7.4
12	Resistance of trenches 30 d	58.2	79.5	67.4	75.0	23.3	7.3

of the waterways: the values in the northern half were increased from 0.8 d to 1.2 d. This gave a small but significant improvement of the calibration criterium for the MHW (run 7 in Table 3.3). After having made this differentiation a systematic sensitivity analysis was performed for the entry resistances of the streams. The values for the whole region were simultaneously changed in the same proportionate manner: the values were increased by 25% (run 8), and then by 60% (run 9). These variations did not cause significant changes in the computed calibration criteria. On the basis of a visual impression the choice was made to set the entry resistance of streams to 1.0 d in the southern half and 1.5 d in the northern half (i.e. the values of run 8). At the 'field' level both the ditches and agricultural drains play a role. It is hard to discern between them when attempting to make adjustments. The choice was made to leave the drainage resistances of the ditches untouched and to do the fine-tuning by introducing agricultural drainage if necessary. This was done with the following procedure:

- the simulated and measured maps of the Mean Highest Watertable are compared at the level of nodal subdomains;
- if the simulated map has a MHW in the class <40 cm b.s.s. (cm below soil surface) and on the measured map it is drier (>40 cm b.s.s.), and the land is used for agriculture, then agricultural drainage is assumed in the nodal subdomain

The procedure has been verified by comparing the calibrated drainage with the known drainage in the Hilver region (Van der Bolt *et al*. 1999). For that part of the region the resemblance between calibrated and known drainage is well over 50% in this study. Considering that the knowledge of existing drainage is known to be partial (many of the locations are unknown) the resemblance is satisfactory as a method of calibration.

In the final phase of the calibration some experiments were done with the drainage resistance of trenches. The default value of 20 d was varied to 10 d and 30 d. The influence of these variations is shown in Figure 3.10 One should take into account that the curve for the measured discharges of the Beerze is at fault for the extreme high values at the bottom end of the exceedance frequency values. The flattening off for exceedance frequencies of less than 0.5 d per year is due to flooding of the weirs that are used for the measurements. If the measurements had been correct the curve would no doubt have followed a similar trajectory

Figure 3.10 Exceedance frequency curves for the Reusel and Beerze, for the final calibrated values of the geohydrological parameters and drainage resistances of streams and ditches, and for three values of the resistances of trenches (10 d, 20 d, and 30 d).

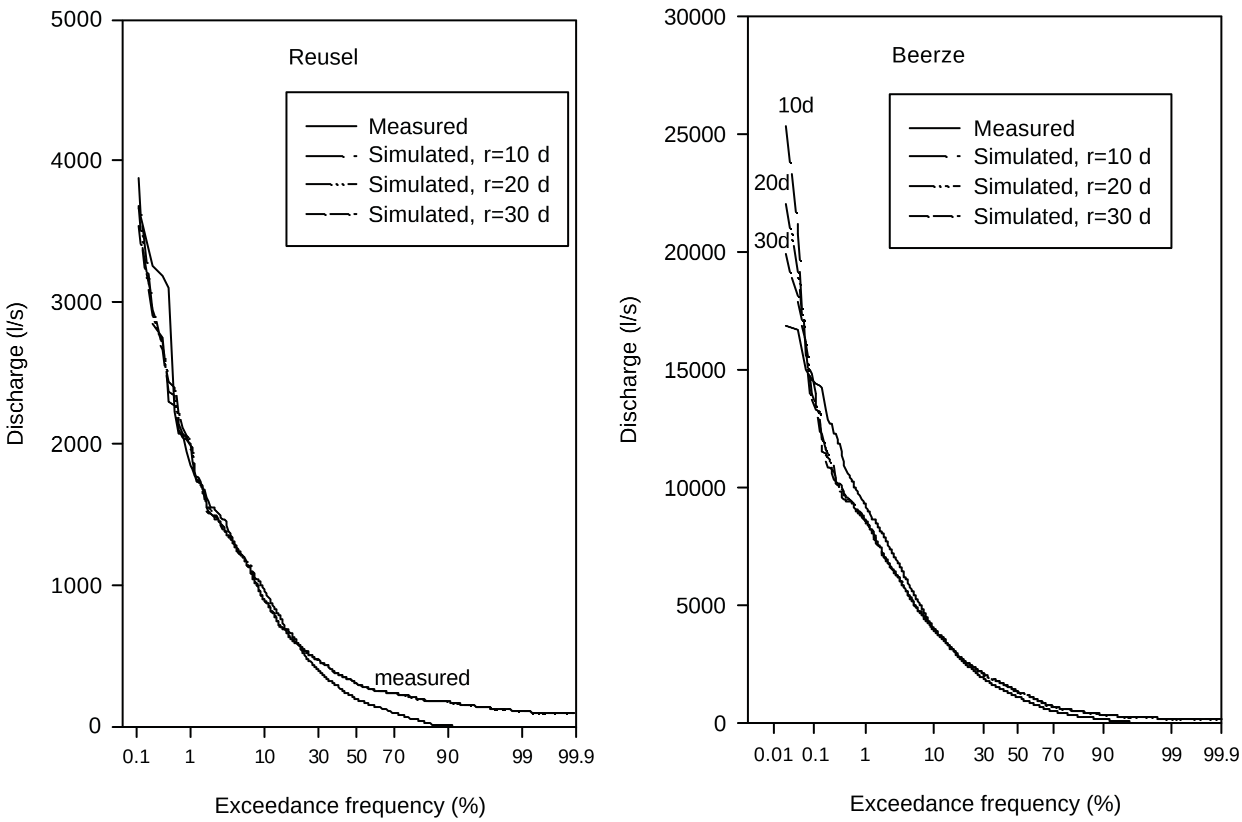

as the one for the Reusel: typically the curve is slightly concave. The choice for the final value (20 d) of the trench drainage resistances was fairly arbitrary. The final simulated map of the Mean Highest Watertable is presented in Figure 3.11.

Figure 3.11 Map of the Mean Highest Watertable (final calibration).

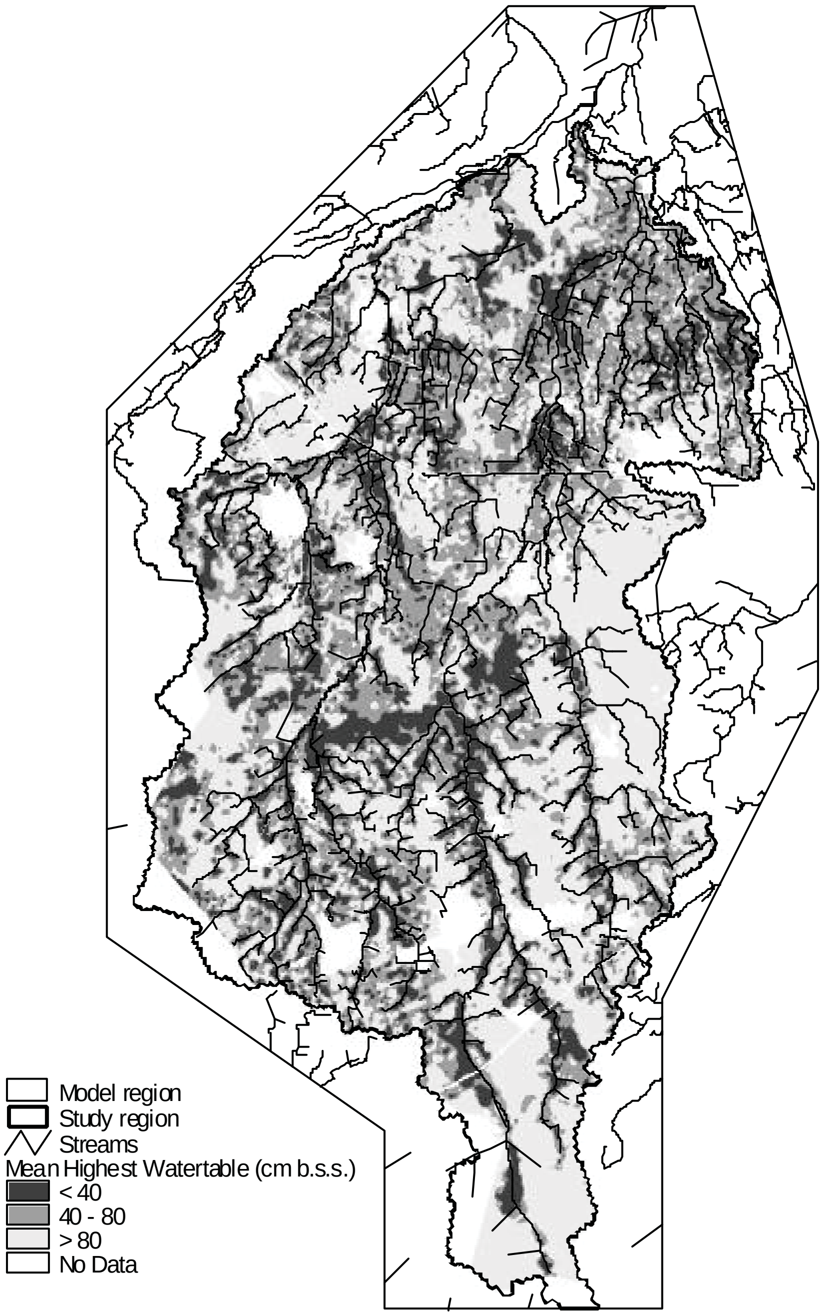

3.3.5 Verification with gauging wells of OLGA-database

The data of the gauging wells of the OLGA-database (NITG-TNO 1994b) have been reserved for the verification of the calibrated model. In Figure 3.12 the deviations between the simulated and measured heads have been plotted in terms of the mean heads per well, for the shallow (layers 1 and 3) and deeper wells separately. As can be seen from the plot on the

Figure 3.12 Differences between means of simulated and measured heads for the shallow wells (in layer 1 and 3, left side of figure) and deep wells (right side).

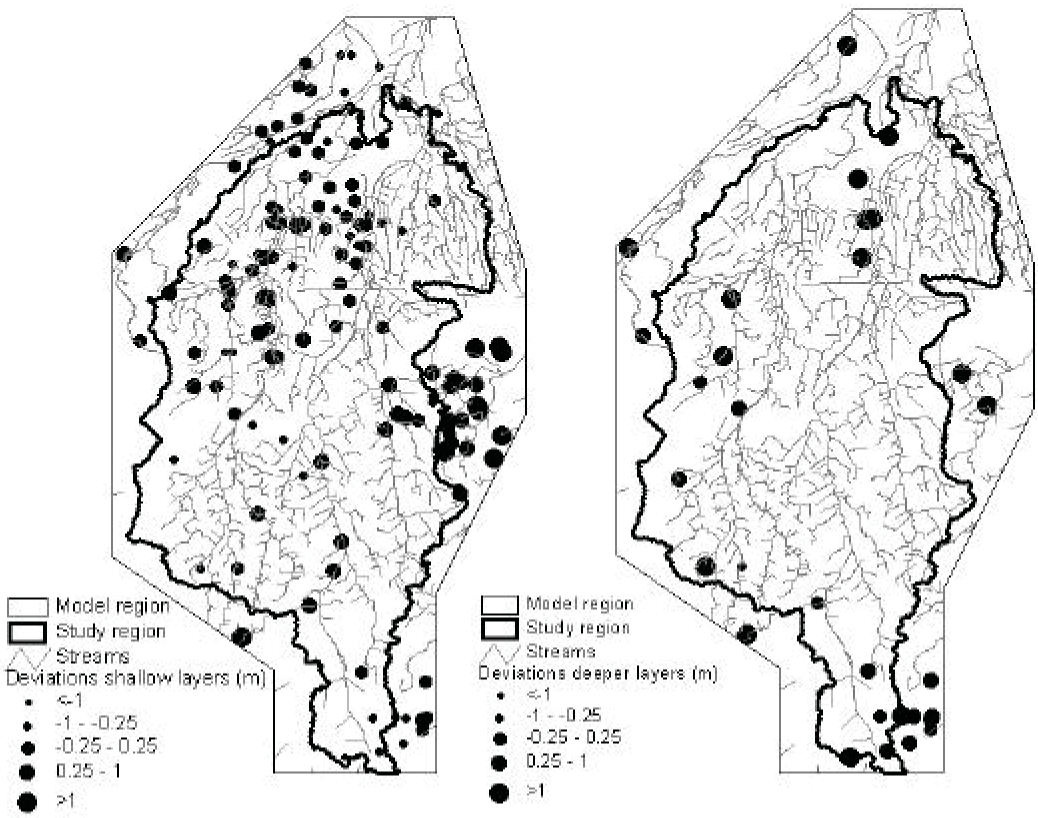

right-hand side the simulated heads for the deep wells are nearly all higher than the measured ones. This means that the heads of the deeper layers can *not* be the cause of the model to underestimate the heads in the phreatic layer. So the underestimation of these heads (that still exists, even after reducing the conductivities during the calibration: see Figure 3.11 compared to the measured map of the Mean Highest Watertable in Figure 3.6a) must out of necessity be caused by circumstances in the upper layers, which are the layers where the conductivities have been reduced in the calibration. The results for the shallow wells in the plot on the left-hand side of Figure 3.12 show some regional tendencies:

Figure 3.13 Examples of simulated vs. measured heads for geohydrological layers 1,3,5,7. The different plots refer to different locations.

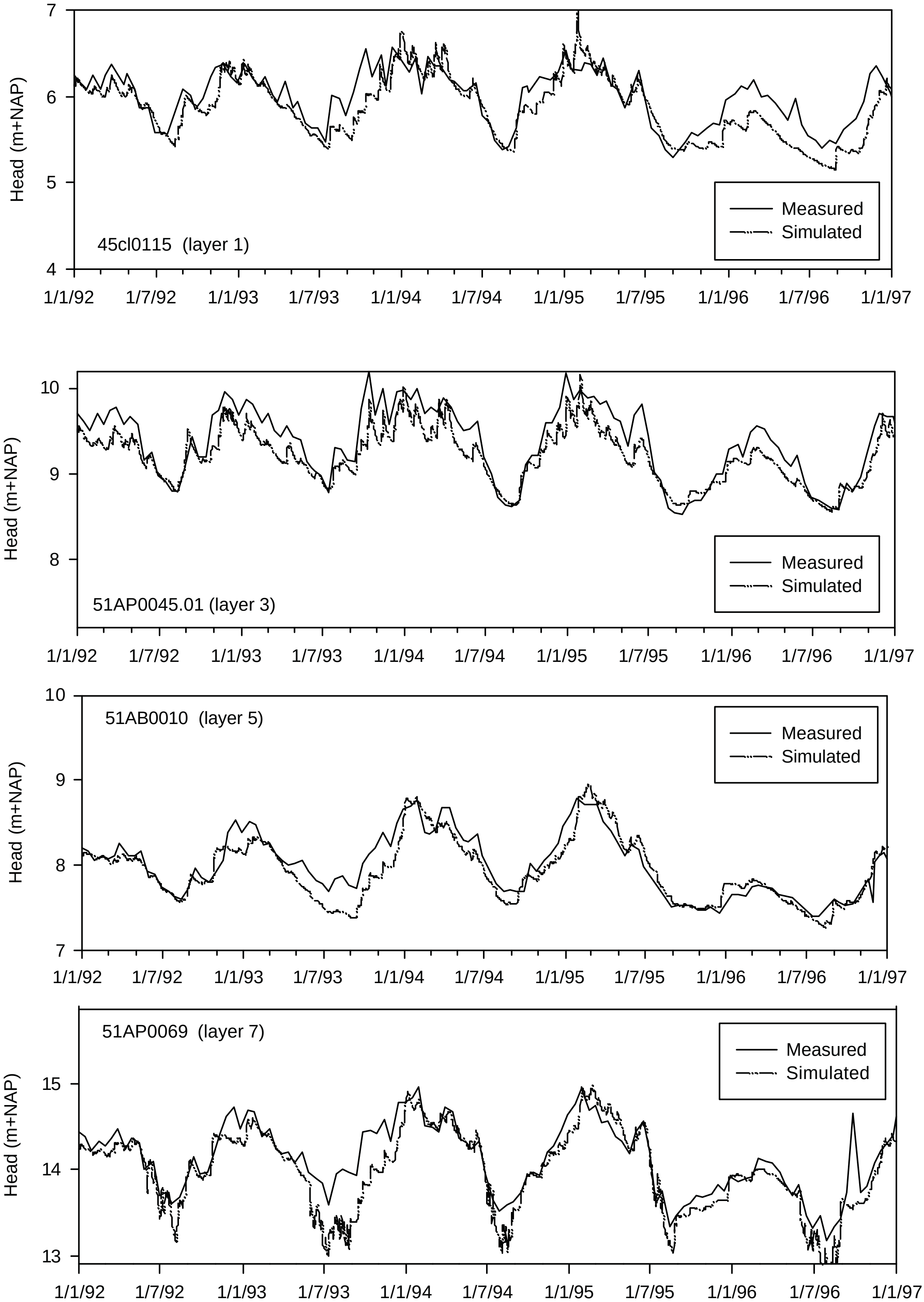

- the cluster of large dots on the right-hand side of the region just outside the border of the study area are in the vicinity of a large drinking water extraction in the third layer. Apparently the model does not properly estimate the drawdown, probably because of too high conductivities in the third layer
- the large dots in the southern half of the study region are nearly all directly next to streams. So either the water levels in the streams or else the drainage resistances are overestimated. The implication is that the underestimation of the groundwater heads in the flanks of the valleys and on the higher grounds is not caused by the conditions near or in the streams. The underestimation must be caused by conductivities that are still too high
- the large dots in the western half of the plot on the left-hand side are in a part of the region that is geologically very complex, with heavy fracturing. Proper simulation of this part of the region would require much more field information

In Figure 3.13 some (good) examples of the comparison between measured and simulated time series of well locations are given.

In the final evaluation of the calibration, it seems likely that further improvement of the model would have required further lowering of the conductivities of the shallow layers. This would not have only further improved the simulation of the Mean Highest Watertable, but would also have improved the simulation of the discharges with an exceedance frequency of around 1 d per year. However, further reduction of the geohydrological conductivities was considered to be out of bounds and therefore not implemented.

3.4 Results for the current situation

In the region it is known that structural changes are taking place. This can also be inferred from Figure 3.4. The dropping of the groundwater head is so systematic that it is not likely to be caused by natural climatological variations of the weather. For simulating conditions that reflect the current situation as well as possible, the final year of the heads in Figure 3.4 has been used for deriving *boundary conditions*: the daily values of the last year have been cyclically repeated for each year of the simulation period.

For simulating the current situation the meteorological data have been used for the period 1984 though 1998, i.e. a period of fifteen years. This period was selected after analyzing a

Figure 3.14 Mean Highest Watertable, simulated for the current situation.

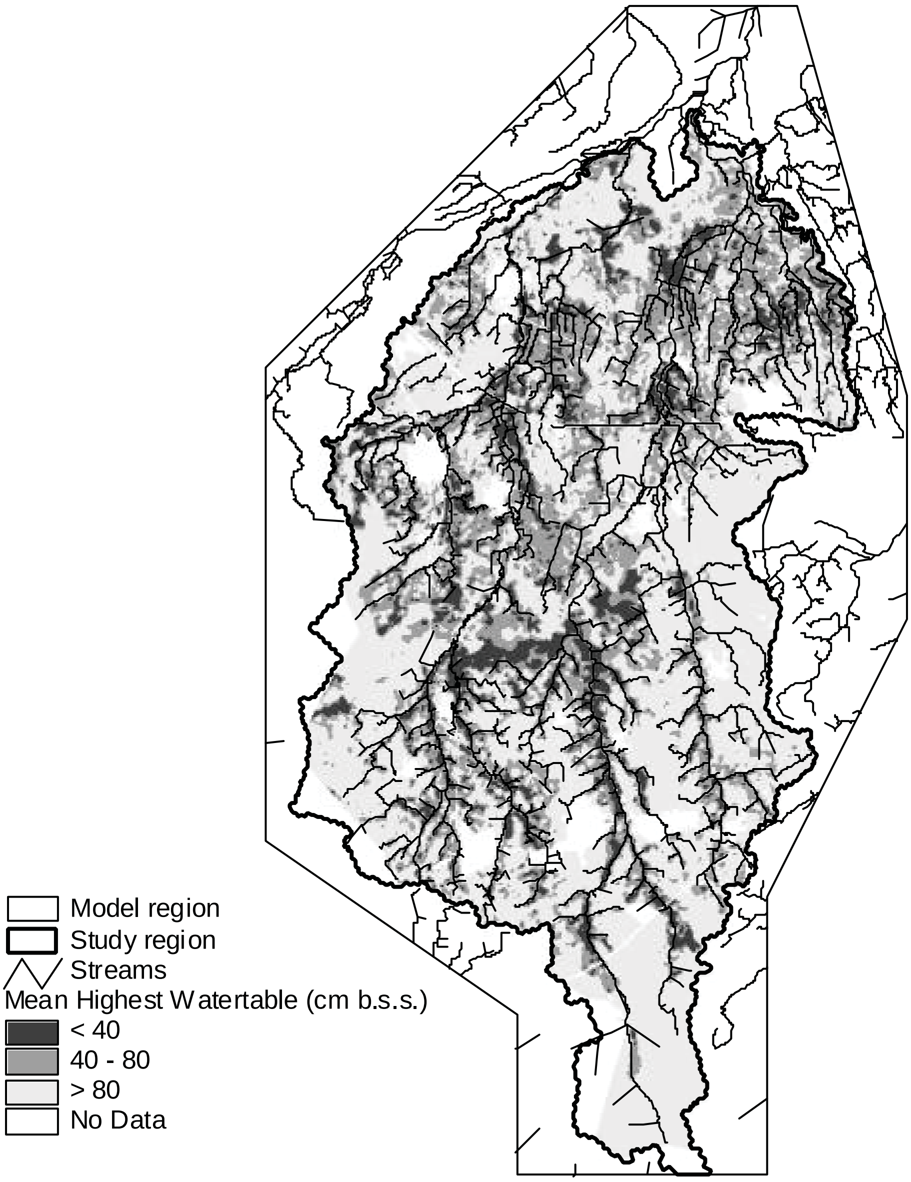

period of 30 years using data of the main meteorological station in the Netherlands. A 'climate' is by definition the weather that occurred during the last 30 years. The reason why the last 30 years could not be used in this study is simply that the daily precipitation data were not available for all the regional gauging stations for so long a period. In Figure 3.14 the simulated map of the Mean Highest Watertable for the current situation is presented. Comparison between the final map for the calibration period (Figure 3.11) shows that the watertables have dropped substantially within a period of 10 years.

Results for the exceedance frequency curves of simulated discharges for the Reusel and Beerze are shown in Figure 3.15. Apart from making a simulation for the current situation, a simulation has been made with the regional precipitation averaged out, with the average simply taken as the arithmetic mean of the six regional precipitation stations. As pointed out in Section 2.2.2, the average precipitation of the Beerze drainage basin is 1.5% less than the arithmetic mean of the weather stations used for the study. By contrast, the precipitation for the Reusel basin is 4.5% higher.

As becomes clear from the plots, the discharge curve for the Beerze is hardly any different. By contrast, the simulated discharges for the Reusel are nearly 20 % less (18%). This is an important fact for the interpretation of scenarios presented in chapters 8-11, because the climate scenarios have been calibrated in terms of the averaged regional precipitation. The implication is that for a certain climate scenario it can be expected that the effect on the discharge will – when compared to the current situation – be roughly 20% lower for the

Figure 3.15 Comparison between frequency exceedance curves of simulated discharges for Reusel and Beerze, for the current situation and for the (hypothetical) situation with the regional precipitation averaged out over 6 regional stations.

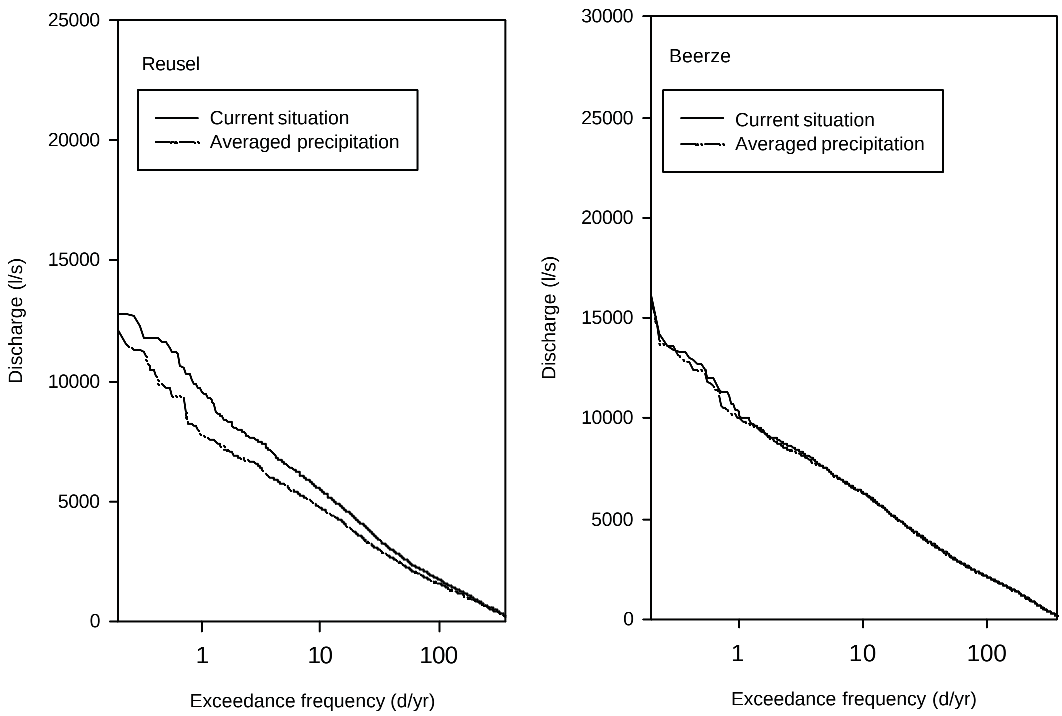

Reusel than for the Beerze: the averaging of the regional precipitation that is implicitly contained in the climate scenarios causes a 20% drop of the discharges for the Reusel, and not for the Beerze. For the interpretation of the scenarios it is a fortunate circumstance that at least for the Beerze there has not been introduced an extra effect due to the regional averaging.